Published OnlineFirst February 28, 2012; DOI: 10.1158/0008-5472.CAN-11-2067

Priority Report

Cancer Research

Bone Marrow Stromal Cells Create a Permissive Microenvironment for Myeloma Development: A New Stromal Role for Wnt Inhibitor Dkk1

Jessica A. Fowler[1], Gregory R. Mundy[2], Seint T. Lwin[2,3], and Claire M. Edwards[1,2,3,4]

Abstract

The rapid progression of multiple myeloma is dependent upon cellular interactions within the bone marrow microenvironment. *In vitro* studies suggest that bone marrow stromal cells (BMSC) can promote myeloma growth and survival and osteolytic bone disease. However, it is not possible to recreate all cellular aspects of the bone marrow microenvironment in an *in vitro* system, and the contributions of BMSCs to myeloma pathogenesis in an intact, immune competent, *in vivo* system are unknown. To investigate this, we used a murine myeloma model that replicates many features of the human disease. Coinoculation of myeloma cells and a BMSC line, isolated from myeloma-permissive mice, into otherwise nonpermissive mice resulted in myeloma development, associated with tumor growth within bone marrow and osteolytic bone disease. In contrast, inoculation of myeloma cells alone did not result in myeloma. BMSCs inoculated alone induced osteoblast suppression, associated with an increase in serum concentrations of the Wnt signaling inhibitor, Dkk1. Dkk1 was highly expressed in BMSCs and in myeloma-permissive bone marrow. Knockdown of Dkk1 expression in BMSCs decreased their ability to promote myeloma and the associated bone disease in mice. Collectively, our results show novel roles of BMSCs and BMSC-derived Dkk1 in the pathogenesis of multiple myeloma *in vivo*. *Cancer Res; 72(9); 2183–9. ©2012 AACR.*

Introduction

The bone marrow is well known to support tumor growth and osteolytic bone disease in multiple myeloma. However, the contributions of this specialized microenvironment during early stages of myeloma development are poorly understood, largely because of the need for *in vivo* experiments that accurately replicate the complexity of tumor–host cell interactions. To address this, we have exploited the unique opportunities provided by the well-characterized 5T Radl myeloma model, in which transplantation of 5T myeloma cells into recipient mice of the specific C57Bl/KaLwRijHsd (KaLwRij) substrain results in propagation of myeloma with many features of the human disease (1). One important feature of the Radl model is that 5T myeloma cells will only grow in syngeneic KaLwRij mice, and not in closely-related C57Bl6 mice. Because there is an emerging role for host fibroblasts in the establishment and progression of solid tumors (2–4), we hypothesized that fibroblasts, or bone marrow stromal cells (BMSCs), from myeloma-permissive KaLwRij mice may promote myeloma development in environments that are otherwise not permissive for myeloma. Furthermore, increasing evidence for elevated Dickkopf 1 (Dkk1) in patients with monoclonal gammopathy of undetermined significance (MGUS; refs. 5–7) suggests a potential role for host-derived Dkk1 in the early stages of myeloma. We used a BMSC line derived from KaLwRij mice to determine the function of BMSCs and BMSC-derived Dkk1 in myeloma pathogenesis *in vivo*.

Authors' Affiliations: Departments of [1]Cancer Biology and [2]Medicine/Clinical Pharmacology, Vanderbilt Center for Bone Biology, Vanderbilt University, Nashville, Tennessee; [3]Nuffield Department of Surgical Sciences; and [4]Nuffield Department of Orthopaedics, Rheumatology and Musculoskeletal Sciences, University of Oxford, Oxford, United Kingdom

Note: Supplementary data for this article are available at Cancer Research Online (http://cancerres.aacrjournals.org/).

Corresponding Author: Claire M. Edwards, Botnar Research Centre, University of Oxford, Old Road, Oxford, OX3 7LD, UK. Phone: 01865-227307, Fax: 01865-227966; Email: claire.edwards@ndorms.ox.ac.uk

doi: 10.1158/0008-5472.CAN-11-2067

Materials and Methods

Cell culture

5TGM1-GFP myeloma cells were cultured as previously described (8). 14M1 BMSCs were originally isolated from KaLwRij mice bearing 5T myeloma. Bone marrow was flushed from long bones, and cells cultured in Dulbecco's Modified Eagle's Medium (DMEM) with 10% fetal calf serum (FCS) and L-glutamine. Media were changed every 3 to 4 days, and adherent cells were maintained in culture. The cell line was generated by continuous growth *in vitro*, with no requirement for cellular or viral immortalizing genes. Aliquots of early passage cells were frozen in 10% dimethyl sulfoxide/90% FCS and stored in liquid nitrogen. ST2 BMSCs were purchased from Riken cell Bank and maintained in DMEM media with 10% FCS and L-glutamine.

Stable cell lines

14M1 BMSCs were transfected with 1 μg Dkk1shRNA or scrambled control (Santa Cruz Biotechnology) using short

Published OnlineFirst February 28, 2012; DOI: 10.1158/0008-5472.CAN-11-2067

hairpin RNA (shRNA) transfection reagent and standard protocols. Cells were cultured in DMEM with 10 μg/mL puromycin. Knockdown of Dkk1 expression was confirmed by ELISA, and cells were continuously cultured in puromycin to maintain knockdown. ST2 BMSCs were transfected with 250 ng full-length Dkk1 cDNA (OriGene) or empty vector control according to the manufacturer's instructions. Cells were cultured in DMEM with 800 μg/mL neomycin. Overexpression of Dkk1 was confirmed by ELISA, and cells were continuously cultured in neomycin to maintain expression.

Differentiation studies

BMSCs were cultured in either control media, osteoblast differentiation media (10 mmol/L β-glycerophosphate, 50 μg/mL ascorbic acid, 10 ng/mL BMP-2), or adipocyte differentiation media (10 nmol/L dexamethasone, 5 μg/mL insulin) for 7 days (osteoblast differentiation) or 10 days (adipocyte differentiation). Osteoblasts were identified by alkaline phosphatase staining, using a BCIP/NBT substrate kit and adipocytes by Oil Red-O staining.

ELISA, western blotting, and flow cytometry

The concentration of Dkk1 in conditioned media or sera was measured by ELISA, according to the manufacturer's instructions (R&D Systems). Sera were assayed for monoclonal mouse $IgG_{2b\kappa}$ paraprotein as described (8). Western blotting and flow cytometry were conducted as previously described, and outlined in Supplemental Data (9).

In vivo studies

Studies were conducted with weight-matched, 8- to 10-week-old female C57BL/KaLwRijHsd (Harlan Netherlands B.V.) or C57Bl6 mice (Harlan U.S.). Studies were approved by the Institution of Animal Care and Use Committee at Vanderbilt University. C57Bl6 or C57Bl/KaLwRij mice were intravenously inoculated with either 10^6 5TGM1-GFP cells alone, 5×10^5 5TGM1-GFP + 5×10^5 14M1 BMSCs or vehicle control (PBS phosphate-buffered saline). In separate studies, C57Bl6 mice were inoculated intravenously with (i) 10^6 5TGM1-GFP, 10^6 ST2 BMSCs, or 5×10^5 5TGM1-GFP + 5×10^5 ST2 BMSCs; (ii) 10^6 14M1 BMSCs, 10^6 14M1-Dkk1KD BMSCs, 5×10^5 5TGM1-GFP + 5×10^5 14M1 BMSCs, 5×10^5 5TGM1-GFP + 5×10^5 14M1-Dkk1KD BMSCs; and (iii) 10^6 5TGM1-GFP, 10^6 ST2 BMSCs, 10^6 ST2-Dkk1 BMSCs, 5×10^5 5TGM1-GFP + 5×10^5 ST2 BMSCs, 5×10^5 5TGM1-GFP + 5×10^5 ST2-Dkk1 BMSCs. In another series of experiments, 5×10^5 5TGM1-GFP, 5×10^5 C4-2b-GFP, or 5×10^5 MDA-231-GFP tumor cells, in the presence or absence of 5×10^5 14M1 BMSCs were injected into the tibias of C57Bl6 mice. GFP-tagged tumor cell growth was measured and quantified using the CRi Maestro system. After the image was obtained, it was spectrally unmixed to remove the background fluorescence. Images were quantified using region of interest analysis software supplied with the Maestro system.

Histology, microcomputed tomography, and histomorphometric analyses

Histomorphometric analysis was conducted to quantify bone volume and osteoclast and osteoblast surface area to bone surface area. Tibias and femurs were formalin fixed, decalcified in 14% EDTA, paraffin-embedded, sectioned along the midsagittal plane in 4 μm thick sections and stained with hematoxylin and eosin. To visualize osteoclasts, sections were stained for TRAP activity. For visualization of tetracycline labeling, spines were fixed in 70% ethanol and embedded in methylmethacrylate without prior decalcification. A total of 6 μm sections were cut and viewed unstained by epifluorescence microscopy. Three nonconsecutive sections were evaluated with Osteomeasure histomorphometry software, as described previously (9). Tibias were fixed in formalin and each bone was scanned at an isotropic voxel size of 12 μm using a microCT40 (CT, computed tomography; SCANCO Medical). Images were analyzed using the SCANCO Medical Imaging Software and AMIRA 3-D graphics software (Mercury Computer Systems) to quantitate cortical bone lesions and trabecular bone volume, as described previously (9). Fluorescent *in situ* hybridization, immunohistochemistry, and immunocytochemistry were carried out as detailed in Supplementary Methods.

Statistical analysis

Statistical significance was determined by a Mann–Whitney *U* test for nonparametric data, or 1-way ANOVA followed by the Tukey posthoc test. Data were considered significant given $P \leq 0.05$. Data are presented as means (± SEM) unless otherwise stated.

Results and Discussion

The importance of the host microenvironment in myeloma is exemplified by the 5T myeloma model, in which KaLwRij mice possess a unique host microenvironment that is permissive for 5T myeloma growth (10). We were able to induce myeloma development in nonpermissive C57Bl6 mice by inoculating 5TGM1 myeloma cells in the presence of BMSCs isolated from KaLwRij mice (14M1 BMSCs). Importantly, myeloma induced by coinoculation of myeloma cells and 14M1 BMSCs had many characteristics of both the original syngeneic KaLwRij model, and human myeloma. Mice showed a time-dependent increase in serum paraprotein concentrations similar to the original KaLwRij model and accumulation of myeloma cells in bone marrow and spleen (Fig. 1A and B). Osteolytic bone disease is a major feature of multiple myeloma, and histomorphometric and microCT analysis confirmed a significant increase in osteolytic lesion number and osteoclast number, meanwhile showing a significant decrease in trabecular bone volume and osteoblast number (Fig. 1C, Supplementary Fig. S1). Histologic analysis revealed that C57Bl6 mice inoculated with 5TGM1 myeloma cells in the presence of 14M1 BMSCs displayed a striking similarity to the original KaLwRij myeloma model, with replacement of bone marrow by myeloma cells, loss of trabecular bone, and erosion through cortical bone (Fig. 1D). Inoculation of 5TGM1 myeloma cells alone into C57Bl6 mice did not result in the development of myeloma, with no significant accumulation of plasma cells within the bone marrow or evidence of osteolytic bone disease. There is increasing evidence from solid tumors to support a role for fibroblasts in tumor progression (11, 12). In contrast to

Published OnlineFirst February 28, 2012; DOI: 10.1158/0008-5472.CAN-11-2067

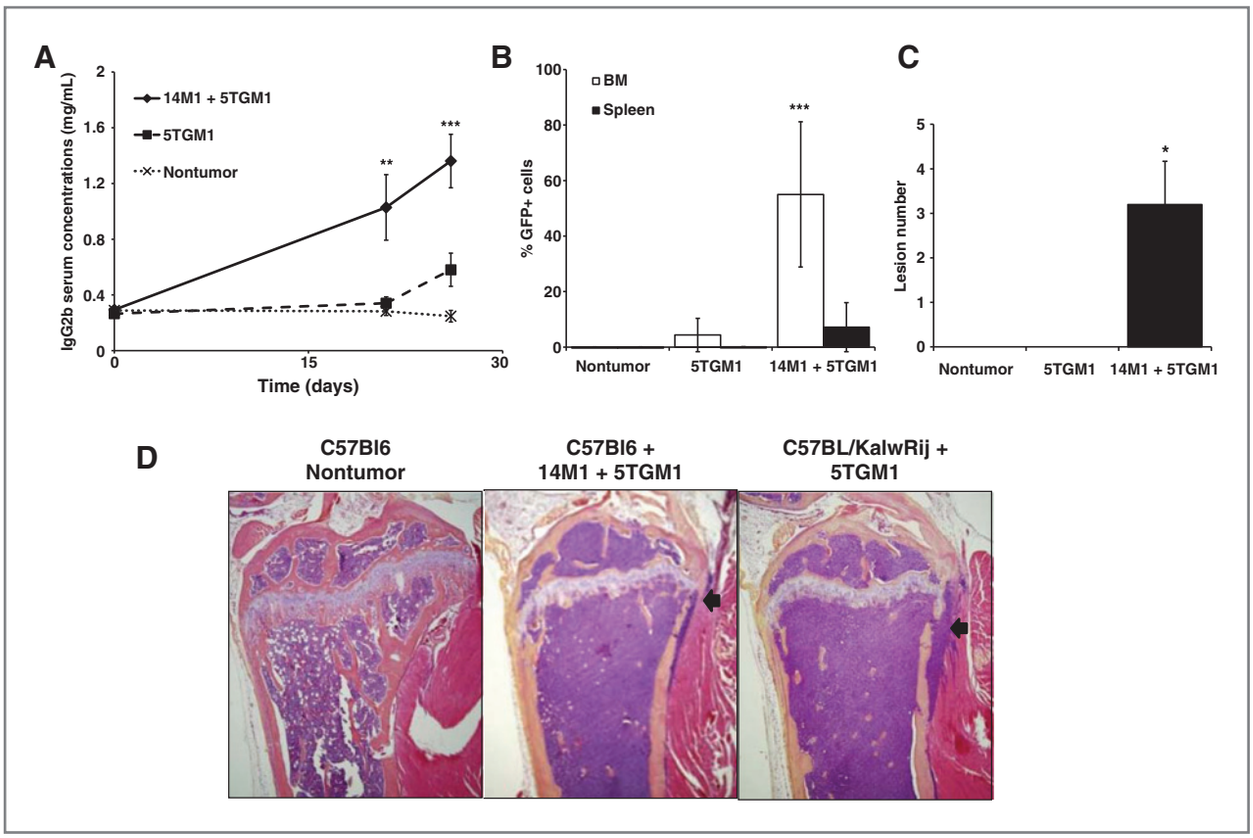

Figure 1. 14M1 BMSCs promote myeloma development in nonpermissive C57Bl6 mice. C57Bl6 mice were inoculated with either 10^6 5TGM1-GFP cells alone, 5×10^5 5TGM1-GFP + 5×10^5 14M1 BMSCs or vehicle control (PBS). Coinoculation of 5TGM1 myeloma cells plus 14M1 BMSCs significantly increased serum $IgG_{2b\kappa}$ concentrations (A) and tumor burden within bone marrow and spleen (B). C, coinoculation of 14M1 BMSCs and 5TGM1 myeloma cells resulted in the development of myeloma bone disease, associated with an increase in osteolytic lesions. D, histologic sections showed the similarity between C57Bl6 mice coinoculated with 14M1 BMSCs and 5TGM1 myeloma cells as compared with the original 5T model, in which KalwRij mice are inoculated with 5TGM1 myeloma cells. Arrows indicate areas where tumor cells have eroded through cortical bone. *, $P < 0.05$; **, $P < 0.01$; ***, $P < 0.001$ as compared with 5TGM1.

previously published studies, in which the fibroblasts were enhancing tumor growth, we have identified a role for fibroblasts or BMSCs whereby the tumor is unable to grow unless the fibroblasts are present, highlighting the critical role of these cells in myeloma pathogenesis.

Coinoculation of 14M1 BMSCs with 5TGM1 myeloma cells resulted in myeloma development in an otherwise nonpermissive microenvironment. In contrast, coinoculation of 5TGM1 myeloma cells with normal ST2 BMSCs had no effect to promote myeloma development in C57Bl6 mice (Fig. 2A), despite engraftment of ST2 cells in the bone marrow (5%–15%). This suggests that the effect of 14M1 BMSCs is specific and not a general effect of all BMSCs. To determine whether the effect of 14M1 BMSCs was specific for myeloma cells, or whether it could promote the growth of other tumor cells, C57Bl6 mice were inoculated directly into the tibia with either 5TGM1 myeloma cells, C4-2b prostate cancer cells, or MDA-231 breast cancer cells in the presence and absence of 14M1 BMSCs. All tumor cells were labeled with GFP. *In vivo* imaging detected tumor burden by GFP expression in only those mice coinoculated with 5TGM1 myeloma cells in the presence of 14M1 BMSCs, showing that 14M1 BMSCs could not promote breast or prostate cancer cell growth in a nonpermissive microenvironment (data not shown). Together, these studies confirm that the effect of the 14M1 BMSCs is both cell type and disease specific.

14M1 BMSCs were originally isolated from myeloma-bearing KaLwRIj mice, and so represent host stromal cells from the permissive KaLwRij bone marrow microenvironment. 14M1 BMSCs expressed both vimentin and fibroblast-specific protein-1, indicative of fibroblasts (Fig. 2B). Immunocytochemistry for FSP-1 showed expression by all cells, confirming that 14M1 BMSCs are comprised entirely of fibroblasts. (Supplementary Fig. S2). Further characterization showed no osteogenic or adipogenic differentiation potential, commonly seen in BMSCs (Fig. 2C). *In vivo* analysis confirmed engraftment of 14M1 BMSCs, with flow cytometric analysis detecting approximately 13% BMSCs in the bone marrow following coinoculation of 14M1 cells labeled with DsRedII with myeloma cells (Supplementary Fig. S3). Inoculation of 14M1 BMSCs was unable to support the growth of human myeloma cells and had no effect on the proportion of B, T, or NK cells suggesting that 14M1 cells were not immunosuppressive (Supplementary Fig. S4). To further characterize the *in vivo* effects of 14M1

Published OnlineFirst February 28, 2012; DOI: 10.1158/0008-5472.CAN-11-2067

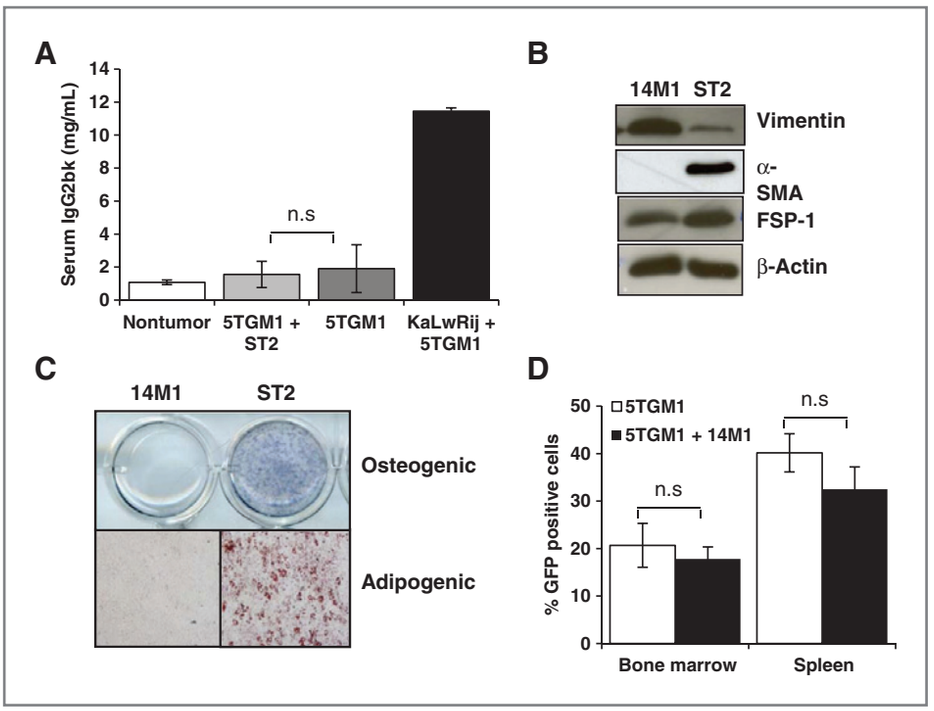

Figure 2. Characterization of 14M1 BMSCs *in vitro* and *in vivo*. C57Bl6 mice were inoculated with either 10^6 5TGM1-GFP cells alone, 5×10^5 5TGM1-GFP + 5×10^5 ST2 BMSCs, or vehicle control (PBS). KaLwRij mice were inoculated with 5TGM1 myeloma cells as a positive control. A, coinoculation of ST2 BMSCs with 5TGM1 myeloma cells had no effect on tumor burden, as measured by serum IgG2bk. B, Western blot analysis showed expression of vimentin and FSP-1 by 14M1 BMSCs. C, in contrast to ST2 BMSCs, 14M1 BMSCs did not differentiate into osteoblasts or adipocytes. KaLwRij mice were inoculated with either 10^6 5TGM1-GFP cells alone, 5×10^5 5TGM1-GFP + 5×10^5 14M1 BMSCs, or vehicle control (PBS). D, coinoculation of 14M1 BMSCs with 5TGM1 myeloma cells had no effect on tumor burden, as measured by serum IgG2bk.

BMSCs, 5TGM1 myeloma cells and 14M1 BMSCs were coinoculated into KaLwRij mice, which are already permissive for 5T myeloma development. Although 5TGM1 myeloma cell inoculation resulted in tumor growth and osteolytic bone disease, the coinoculation of 14M1 BMSCs did not further increase tumor burden in bone marrow or spleen (Fig. 2D) or osteolysis (data not shown), suggesting that the 14M1 BMSCs were not acting directly on the myeloma cells to increase myeloma growth.

The inability of 14M1 BMSCs to promote myeloma in an already permissive environment suggested that the cells might instead act directly on the host microenvironment to render it

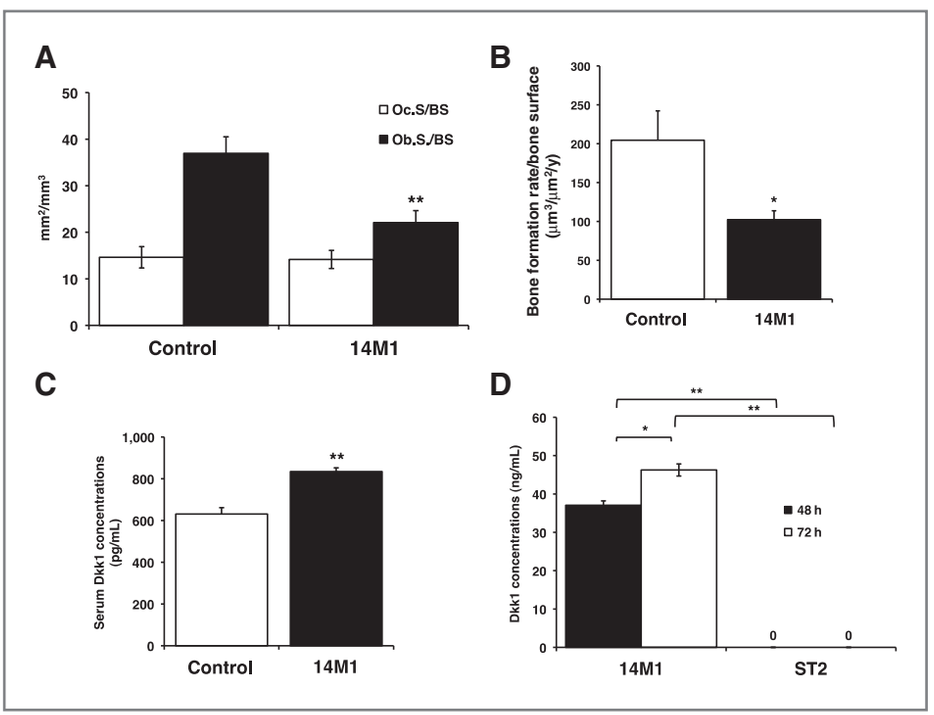

Figure 3. 14M1 BMSCs have direct effects to decrease bone formation. C57Bl6 mice were inoculated with 10^6 14M1 BMSCs and sacrificed after a period of 4 weeks. Inoculation of 14M1 BMSCs had no effect on osteoclast numbers, but significantly decreased osteoblast numbers (A), rates of bone formation (B), and increased serum concentrations of Dkk1 (C). D, 14M1 BMSCs secrete high concentrations of Dkk1. *, $P < 0.05$; **, $P < 0.01$, as compared with control.

Published OnlineFirst February 28, 2012; DOI: 10.1158/0008-5472.CAN-11-2067

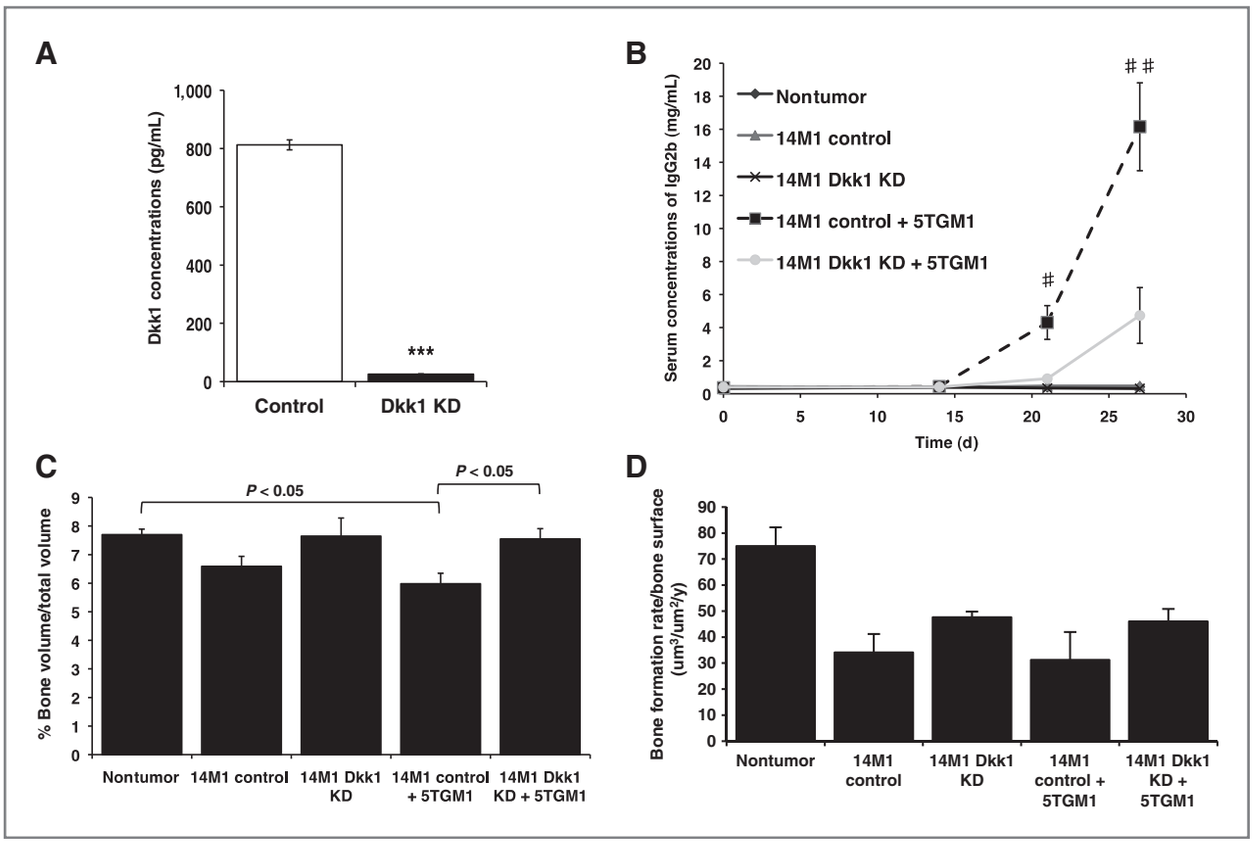

Figure 4. BMSC-derived Dkk1 creates a microenvironment that is permissive for myeloma development. A, 14M1 BMSCs were stably transfected with Dkk1 shRNA (Dkk1 KD) or scrambled control (control), resulting in a significant reduction in secretion of Dkk1. Coinoculation of C57Bl6 mice with 5TGM1 myeloma cells plus 14M1 Dkk1 KD cells resulted in a significant decrease in tumor burden, as measured by serum $IgG_{2bκ}$ (B), and increase in trabecular bone volume (C) and bone formation rates (D) as compared with 5TGM1 myeloma cells plus 14M1 control cells. *, $P < 0.05$; **, $P < 0.01$; ***, $P < 0.001$ as compared with control. #, $P < 0.05$; ##, $P < 0.01$ as compared with 14M1 control + 5TGM1.

permissive for myeloma. To investigate this, we inoculated C57Bl6 mice with 14M1 BMSCs alone. After 4 weeks, we detected a 23.4% decrease in trabecular bone (control, 7.38 ± 1.50 vs. 14M1 BMSCs, 5.65 ± 2.13), associated with a significant decrease in osteoblast number and bone formation rates, but no change in osteoclast number (Fig. 3A and B). In control experiments, inoculation of ST2 BMSCs was found to have no effect on trabecular bone volume, bone cell number, or bone formation rates (data not shown). In support of a decrease in trabecular bone volume contributing to myeloma development, KaLwRij mice were also found to have a significant reduction in trabecular bone volume (Supplementary Fig. S5) when compared with age- and sex-matched C57Bl6 mice.

Because a major mediator of osteoblast suppression in myeloma bone disease is Dkk1 (13–15), we measured Dkk1 serum concentrations, and observed a significant increase in C57Bl6 mice inoculated with 14M1 BMSCs, as compared with either C57Bl6 or C57Bl6 mice inoculated with ST2 BMSCs (Fig. 3C). 14M1 BMSCs were found to express high concentrations of Dkk1 *in vitro* (Fig. 3D), and investigation of Dkk1 expression in myeloma-permissive KaLwRij mice showed a significant 160.8% increase in Dkk1 serum concentrations ($P < 0.05$) and increased expression of Dkk1 in KaLwij BMSCs (Supplementary Fig. S6), suggesting a possible role for Dkk1 in myeloma-permissive microenvironments. In support of this, immunohistochemistry revealed an increase in Dkk1 expression within the bone marrow of mice inoculated with 14M1 BMSCs alone, as compared with nontumor-bearing mice (Supplementary Fig. S7). Therefore, we determined the contribution of BMSC-derived Dkk1 in myeloma pathogenesis *in vivo*. 14M1 BMSCs were stably transfected with Dkk1 shRNA or scrambled control, and knockdown of Dkk1 expression was confirmed by ELISA (Fig. 4A). Knockdown of Dkk1 expression had no effect on the growth rate of 14M1 BMSCs *in vitro* (data not shown). C57Bl6 mice were inoculated with 5TGM1 myeloma cells in the presence of either 14M1 scrambled control BMSCs or 14M1 DKK1 knockdown BMSCs. Those mice inoculated with 5TGM1 cells in the presence of 14M1 DKK1 knockdown BMSCs had a significant reduction in tumor development, as measured by serum IgG2bk titers, when compared with mice coinoculated with 5TGM1 myeloma cells and 14M1 scrambled control BMSCs (Fig. 4B). Knockdown of Dkk1 expression in the 14M1 BMSCs prevented the reduction in trabecular bone volume observed in those mice coinoculated with 5TGM1 myeloma cells and 14M1 BMSCs (Fig. 4C),

Published OnlineFirst February 28, 2012; DOI: 10.1158/0008-5472.CAN-11-2067

and this was associated with an increase in rates of bone formation (Fig. 4D). ST2 BMSCs were stably transfected to overexpress Dkk1, however coinoculation of these BMSCs with 5TGM1 myeloma cells in C57Bl6 mice did not result in myeloma (Supplementary Fig. S8).

Dkk1 plays a key role in the osteoblast suppression of myeloma bone disease, but the majority of studies to date have focused upon the role of myeloma-derived Dkk1 (13, 15). Stromal cells and osteoblasts are known sources of Dkk1 (16, 17), and this study provides compelling evidence for a key role of stromal-derived Dkk1 to promote myeloma development. There is increasing evidence to suggest that cells of the bone marrow microenvironment are altered in MGUS, and that Dkk1 is increased in patients with MGUS, associated with a loss of trabecular bone (5–7). In support of this, our studies show increased host-derived Dkk1 in myeloma-permissive KaLwRij mice that is associated with a significant reduction in trabecular bone volume. Furthermore, we have discovered a novel role of BMSCs to promote myeloma establishment and progression in an otherwise nonpermissive environment. This is mediated, in part, through stromal-derived Dkk1, however the inability of overexpression of Dkk1 in normal BMSCs to support myeloma development reveals that Dkk1 alone is not permissive for myeloma development and suggests a requirement for additional factors. Furthermore, although Dkk1 expression is undetectable *in vitro*, 5TGM1 myeloma cells do express Dkk1 *in vivo*, raising the possibility that tumor-derived Dkk1 may compensate for a loss in host-derived Dkk1 (Supplementary Fig. S7).

It is intriguing to speculate whether the effect of 14M1 BMSCs is associated with a generalized osteoblast suppression that renders the bone marrow microenvironment favorable for myeloma. In support of this, recent studies have implicated changes in the bone marrow, associated with bone loss, that contribute to the initiation of hematopoietic cell diseases (18–20). An anti-human Dkk1 neutralizing antibody (BHQ880) is currently in phase I/II clinical trials in multiple myeloma, for the treatment of the osteolytic bone disease. This study identifies a novel role for stromal-derived Dkk1 in myeloma pathogenesis, by rendering the host microenvironment favorable for myeloma growth and development. Therefore, targeting Dkk1, such as with a neutralizing antibody, may have additional applications, including preventing myeloma progression during early stages of disease development. Collectively, our studies reveal the importance of host-derived Dkk1 and BMSCs in the pathogenesis of myeloma *in vivo*, highlighting the importance of changes in the local bone marrow microenvironment in the early stages of myeloma development.

Disclosure of Potential Conflicts of Interest

No potential conflicts of interest were disclosed.

Authors' Contributions

Conception and design: J.A. Fowler, G.R. Mundy, C.M. Edwards
Development of methodology: J.A. Fowler, C.M. Edwards
Acquisition of data: J.A. Fowler, S.T. Lwin
Analysis and interpretation of data: J.A. Fowler, C.M. Edwards
Writing, review, and/or revision of the manuscript: J.A. Fowler, C.M. Edwards
Administrative, technical, or material support: J.A. Fowler
Study supervision: J.A. Fowler, C.M. Edwards

Grant Support

This work was supported by National Cancer Institute through R01 CA 137116 (C.M. Edwards) and P01 CA-40035 (G.R. Mundy) and by the Leukemia Research Foundation (C.M. Edwards) and the Elsa U. Pardee Foundation (C.M. Edwards); the Vanderbilt University Institute of Imaging Science and the Vanderbilt Medical Center (VMC) Flow Cytometry Shared Resource. The VMC Flow Cytometry Shared Resource is supported by the Vanderbilt Ingram Cancer Center (P30 CA68485) and the Vanderbilt Digestive Disease Research Center (DK058404).

Received June 17, 2011; revised February 2, 2012; accepted February 13, 2012; published OnlineFirst February 28, 2012.

References

1. Radl J, Croese JW, Zurcher C, Van Den Enden-Vieveen MHM, Margreet de Leeuw A. Animal model of human disease; multiple myeloma. Am J Pathol 1988;132:593–7.
2. Hayward SW, Wang Y, Cao M, Hom YK, Zhang B, Grossfeld GD, et al. Malignant transformation in a nontumorigenic human prostatic epithelial cell line. Cancer Res 2001;61:8135–42.
3. Bhowmick NA, Chytil A, Plieth D, Gorska AE, Dumont N, Shappell S, et al. TGF-beta signaling in fibroblasts modulates the oncogenic potential of adjacent epithelia. Science 2004;303:848–51.
4. Parrinello S, Coppe JP, Krtolica A, Campisi J. Stromal-epithelial interactions in aging and cancer: senescent fibroblasts alter epithelial cell differentiation. J Cell Sci 2005;118:485–96.
5. Ng AC, Khosla S, Charatcharoenwitthaya N, Kumar SK, Achenbach SJ, Holets MF, et al. Bone microstructural changes revealed by high-resolution peripheral quantitative computed tomography imaging and elevated Dkk1 and MIP-1alpha levels in patients with MGUS. Blood 2011;118:6529–34.
6. Corre J, Mahtouk K, Attal M, Gadelorge M, Huynh A, Fleury-Cappellesso S, et al. Bone marrow mesenchymal stem cells are abnormal in multiple myeloma. Leukemia 2007;21:1079–88.
7. Todoerti K, Lisignoli G, Storti P, Agnelli L, Novara F, Manferdini C, et al. Distinct transcriptional profiles characterize bone microenvironment mesenchymal cells rather than osteoblasts in relationship with multiple myeloma bone disease. Exp Hematol 2010;38:141–53.
8. Dallas SL, Garrett IR, Oyayobi BO, Dallas MR, Boyce BF, Bauss F, et al. Ibandronate reduces osteolytic lesions but not tumour burden in a murine model of myeloma bone disease. Blood 1999;93:1697–706.
9. Edwards CM, Edwards JR, Lwin ST, Esparza J, Oyajobi BO, McCluskey B, et al. Increasing Wnt signaling in the bone marrow microenvironment inhibits the development of myeloma bone disease and reduces tumor burden in bone *in vivo*. Blood 2008;111:2833–42.
10. Radl J, de Glopper E, Schuit HER, Zurcher C. Idiopathic paraprotienemia: II. Transplantation of the paraprotein-producing clone from old to young C587Bl/KaLwRij mice. J Immunol 1979;122:609–13.
11. Erez N, Truitt M, Olson P, Arron ST, Hanahan D. Cancer-associated fibroblasts are activated in incipient neoplasia to orchestrate tumor-promoting inflammation in an NF-kappaB-dependent manner. Cancer Cell 2010;17:135–47.
12. Orimo A, Gupta PB, Sgroi DC, Arenzana-Seisdedos F, Delaunay T, Naeem R, et al. Stromal fibroblasts present in invasive human breast carcinomas promote tumor growth and angiogenesis through elevated SDF-1/CXCL12 secretion. Cell 2005;121:335–48.
13. Tian E, Zhan F, Walker R, Rasmussen E, Ma Y, Barlogie B, et al. The role of the Wnt-signaling antagonist in the development of osteolytic lesions in multiple myeloma. N Engl J Med 2003;349:2483–94.
14. Yaccoby S, Ling W, Zhan F, Walker R, Barlogie B, Shaughnessy JD Jr. Antibody-based inhibition of DKK1 suppresses tumor-induced bone

Published OnlineFirst February 28, 2012; DOI: 10.1158/0008-5472.CAN-11-2067

resorption and multiple myeloma growth *in vivo*. Blood 2007;109: 2106–11.

15. Heath DJ, Chantry AD, Buckle CH, Coulton L, Shaughnessy JD Jr, Evans HR, et al. Inhibiting Dickkopf-1 (Dkk1) removes suppression of bone formation and prevents the development of osteolytic bone disease in multiple myeloma. J Bone Miner Res 2009;24: 425–36.
16. Gregory CA, Gunn WG, Reyes E, Smolarz AJ, Munoz J, Spees JL, et al. How Wnt signaling affects bone repair by mesenchymal stem cells from the bone marrow. Ann N Y Acad Sci 2005;1049:97–106.
17. Morvan F, Boulukos K, Clement-Lacroix P, Roman Roman S, Suc-Royer I, Vayssière B, et al. Deletion of a single allele of the Dkk1 gene leads to an increase in bone formation and bone mass. J Bone Miner Res 2006;21:934–45.
18. Walkley CR, Olsen GH, Dworkin S, Fabb SA, Swann J, McArthur GA, et al. A microenvironment-induced myeloproliferative syndrome caused by retinoic acid receptor gamma deficiency. Cell 2007;129: 1097–110.
19. Walkley CR, Shea JM, Sims NA, Purton LE, Orkin SH. Rb regulates interactions between hematopoietic stem cells and their bone marrow microenvironment. Cell 2007;129:1081–95.
20. Raaijmakers MH, Mukherjee S, Guo S, Zhang S, Kobayashi T, Schoonmaker JA, et al. Bone progenitor dysfunction induces myelodysplasia and secondary leukaemia. Nature 2010;464:852–7.

Cancer Research
The Journal of Cancer Research (1916–1930) | The American Journal of Cancer (1931–1940)

AACR American Association for Cancer Research

Bone Marrow Stromal Cells Create a Permissive Microenvironment for Myeloma Development: A New Stromal Role for Wnt Inhibitor Dkk1

Jessica A. Fowler, Gregory R. Mundy, Seint T. Lwin, et al.

Cancer Res 2012;72:2183-2189. Published OnlineFirst February 28, 2012.